



## An Experimental and Analytical Study on Alccofine Based High Strength Concrete

B. Sagar\*, M. V. N. Sivakumar

Department of Civil Engineering, National Institute of Technology Warangal, Telangana, India

### PAPER INFO

#### Paper history:

Received 01 December 2019

Received in revised form 09 February 2020

Accepted 07 March 2020

#### Keywords:

Alccofine

High Strength Concrete

Young's Modulus

Water Absorption and Porosity

Energy Absorption Capacity

Integral Absolute Error

### ABSTRACT

The use of supplementary cementitious materials (SCMs) in concrete manufacturing is considered as financial, technical and environmental benefit. In this regard, this paper presents the experimental and analytical study of high strength concrete (HSC) with alccofine-1203 (alccofine) and fly ash as partial replacements to cement. A total of seven mixes were prepared with different percentages of alccofine (4-14%). The prepared concrete mixes were experimentally tested for slump, compressive, flexural and split tensile strengths for 7, 28, and 56-days curing ages. Uniaxial stress-strain behavior, and water absorption and porosity were evaluated at 28-days curing age. Young's modulus, energy absorption capacity (EAC) and integral absolute error (IAE) were assessed analytically. From the test results, it was observed that the replacement of cement with alccofine significantly improved the workability of the concrete. Among all the mixes, the mix with 10% alccofine content exhibited good behavior in all the investigated parameters. The alccofine incorporation was found to have a negative effect on the behavior of HSC beyond 10% replacement in all the investigated parameters. Based on the experimental compressive strength results, empirical relations were proposed to predict the flexural and split tensile strengths. The proposed empirical relations have the lowest IAE (3.29 and 3.32% for flexural and split tensile strength) in comparison with ACI-318, IS 456 and empirical relations proposed by earlier researchers.

doi: 10.5829/ije.2020.33.04a.03

## 1. INTRODUCTION

Along with increase in population, the consumption of concrete has become the second largest material consumed next to water in recent years. As the need for concrete is increasing and continuing to increase, to meet the demand of construction industry, there has been continuous depletion of natural resources such as calcareous and argillaceous materials for the production of Portland cement. This is having negative impact on environment with continuous digging of natural resources and release of large quantities of carbon dioxide from the cement production plants into the atmosphere [1]. On the other side, the continuously generated waste from industries are also substantially increasing. For these reasons, especially from the last decade, concrete industries have received a lot of attention on the use of alternative cementitious materials to develop concrete in sustainable approach. The use of supplementary cementitious materials (SCMs) as partial

or total replacement to cement in manufacturing of concrete is considered one of the most important technological innovations in concrete manufacturing industry and use of SCMs has financial, and environmental benefits [2]. These recent innovations in civil engineering construction field has seen increasing demand to produce new types of concrete with better-quality properties. HSC can be considered one of the examples of such concrete, owing to superior properties like higher strength, toughness, density and durability than conventional concrete [3]. In line with the rapid advancement of concrete technology and use of pozzolans as SCMs, the ability to produce HSC has increased accordingly [3, 4]. The use of SCMs such as fly ash, metakaolin, and rice husk ash, copper slag, ground granulated blast furnace slag (GGBS), marble powder etc., makes it affordable for the construction industry due to reduced cost. Addition of these SCMs are also found to be advantageous in the cement based grouting application [5-7].

\*Corresponding Author Email: [bsagar006@student.nitw.ac.in](mailto:bsagar006@student.nitw.ac.in) (B. Sagar)

Alcofine is the latest slag based micro fine mineral admixture used as SCM for concrete and mortar. It is an eco-friendly material based on low calcium silicate that consists of a high amount of glass content with high reactivity. It is a highly processed material obtained from GGBS with ultra-fine particles with a fineness of 12000  $\text{cm}^2/\text{g}$  obtained through controlled granulation process resulted in unique chemistry [8-10]. In recent investigations, Sharma [8] attempted to replace Portland Pozzolana Cement (PPC) with optimum 15% of alcofine in HSC and succeeded. The relationship between alcofine based HSC cube compressive strength and cylindrical compressive strength was evaluated by Saurav and Gupta [11]. Narendra and Meena [12] concluded that replacement of cement with combination of fly ash and alcofine resulted in the development of superior eco-friendly concrete.

In this paper, an attempted has been made to find the optimal dose of alcofine as a replacement for cement in the development of HSC. In addition, the study aimed to identify the influence of alcofine on workability, mechanical properties such as compressive, split tensile and flexural strengths; water absorption and porosity and uniaxial stress-strain behavior of HSC is experimentally evaluated. The influence of alcofine addition on Young's modulus and energy absorption capacity of HSC is analytically evaluated.

## 2. EXPERIMENTAL WORK

The research methodology followed in this study is shown in Figure 1.

**2. 1. Constituent Material Properties**  
Ordinary Portland cement of 53 grade with specific gravity of 3.12 was used in this study in accordance with

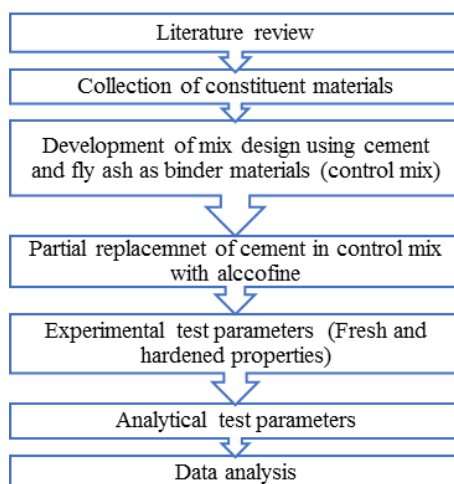


Figure 1. Research Methodology flow chart

IS: 12269-2013 [13]. Fly ash used in this study is classified as alumina silicate fly ash, popularly known as class F fly ash that complies with IS:3812-Part-I [14]. The scanning electron microscope (SEM) image of fly ash is shown in Figure 2 and the particles of fly ash were found to be glassy spheres. The specific surface area of fly ash is 360  $\text{cm}^2/\text{g}$  with a specific gravity of 2.26. Alcofine used in this study is classified as Alcofine-1203 that complies with IS:456-2000 [15] and IS:12089-1987 [16]. The SEM image of alcofine is presented in Figure 3 and the particles of alcofine were found to be irregular in shape with sharp edges. The specific surface area of alcofine is 1200  $\text{cm}^2/\text{g}$ , specific gravity is 2.7. The particle size distribution of alcofine is shown in Figure 4. The chemical properties of cement, fly ash and alcofine are given in Table 1. Natural river sand and crushed granite were used as fine aggregates (Zone-II) and course aggregates in this study in accordance with IS:383-1970 [17]. Portable water was used for manufacturing of concrete and curing conforming to IS:456-2009 [15]. To increase the performance of HSC, masterglennium SKY 8233, a high performance superplasticizer based on polycarboxylic ether was used in this study confirming to IS:9103-1999 [18].

TABLE 1. Chemical compositions of binder materials

Oxide Constituents	Composition (%)		
	Cement	Fly ash	Alcofine
Aluminum oxide ( $\text{Al}_2\text{O}_3$ )	4.72	28.15	24.57
Silicon dioxide ( $\text{SiO}_2$ )	22.53	61.55	37.53
Magnesium oxide ( $\text{MgO}$ )	1.46	1.02	5.23
Calcium oxide ( $\text{CaO}$ )	63.68	2.35	29.46
Ferric Oxide ( $\text{Fe}_2\text{O}_3$ )	3.38	4.22	0.92
Sulphur trioxide ( $\text{SO}_3$ )	1.32	0.25	0.18
Sodium oxide ( $\text{Na}_2\text{O}$ )	0.37	0.2	0.032
Potassium oxide ( $\text{K}_2\text{O}$ )	0.71	1.75	0.61
Loss of ignition (LOI)	0.75	0.3	0.58

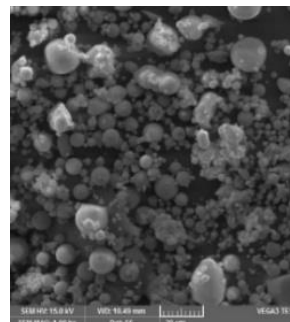


Figure 2. SEM image of fly ash

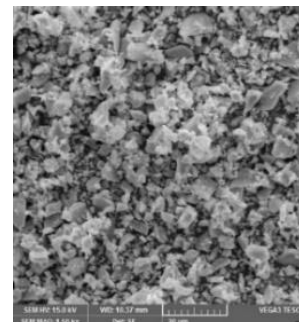


Figure 3. SEM image of alcofine

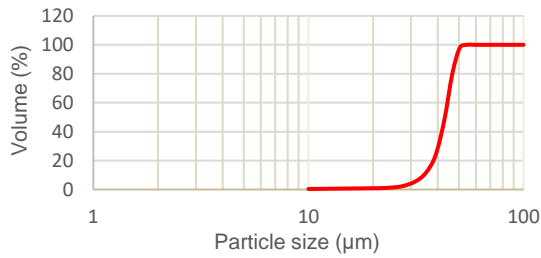


Figure 4. Particle size distribution of alccofine

## 2. 2. Manufacturing of Concrete

### 2 .2. 1. Mix Proportion and Mixes

The mix proportion of 1:1.22:1.58 is developed for the present study according to guidelines given in IS:10262-2009 [19]. A total of 7 mixes were prepared with water/binder ratio of 0.26. As alccofine is rich in calcium oxide and aluminum oxide, the combination of alccofine with cement alone in the manufacturing of HSC may lead to the undesirable behaviour. In order to avoid such undesirability and enhance the performance HSC such as workability, cohesiveness and segregation and bleeding, a 20% of class-F fly ash was used to replace the cement in control mix as well as in all the alccofine based mixes. Out of 7 mixes, CM is a control mix with 80% cement, 20% fly ash and 0% alccofine while the remaining 6 mixes are based on alccofine. On the basis of cement replacement with alccofine, the remaining 6 mixes were named from M-AF4 to M-AF14 are mentioned in Table 2. In the given mix designation, M stands for Mix, AF stands for alccofine and numerical digit stands for percentage replacement of cement with alccofine. CM consist of total binder weight as 600 kg/m<sup>3</sup>. 0.725% of total weight of binder materials is used as dosage of superplasticizer.

### 2. 3. Mixing, Cast and Curing of Concrete Specimens

The guidelines given in IS 456-2000 [15] were followed for concrete mixing. Table vibrator was used to ensure well compaction of concrete in the moulds. After 24 hours of cast, all the specimens were

TABLE 2. Proportion of binder content (kg/m<sup>3</sup>)

Mix designation	Cement (C)	Fly ash (FA)	Alccofine (AF)	% (C:FA:AF)
M-C	480	120	-	80:20:0
M-AF4	456	120	24	76:20:4
M-AF6	444	120	36	74:20:6
M-AF8	432	120	48	72:20:8
M-AF10	420	120	60	70:20:10
M-AF12	408	120	72	68:20:12
M-AF14	396	120	84	66:20:14

demould and then cured in water at a room temperature of  $27 \pm 2$  °C until the test age. The specimens for mechanical properties were tested 7, 28 and 56-days strength and specimens for stress-strain behavior and water absorption were tested for 28-days strength.

### 2. 4. Test Specimens and Methods

A 3000 kN capacity Tinnus-Olsen test machine was used to measure the compressive and split tensile strengths. The compressive strength of cube specimens of size 100×100×100 mm was used and evaluated at 140 kg/cm<sup>2</sup>/min loading rate according to IS:516 [20] and the split tensile strength of cylindrical specimens of size 200×100×100 mm was used and evaluated at 1.5MPa/min loading rate according to IS:5816 [21]. A 200 kN universal testing machine was used to measure the flexural strength, a two point bending test was carried out on specimens of size 500×100×100 mm at 180 kg/min loading rate according to IS:516 [20]. In accordance to ASTM C469 [22], uniaxial compression stress-strain behavior of concrete is evaluated on specimens of size 200×100×100 mm using a 2000kN capacity compression testing machine at a loading rate of 4.5kN/s. Under the load, the axial deformations developed in the specimens with respect to applied load was noted from the data acquisition system (DAC) by means of connected Linearly Varying Displacement Transducers (LVDTs) and load cell, as shown in Figure 5. The loading process on the specimen is shown in Figure 6. Water absorption and porosity test was performed on concrete specimens of size 100 cubic mm at 28 days according to ASTM C642-13 [23]. The water absorption was reported as a percentage of weight increase due to the absorption at dry weight. The porosity of the specimens was also evaluated for control and alccofine based mixes and presented in terms of percentage.

## 3. RESULTS AND DISCUSSION

### 3. 1. Rheological Property

The effect of alccofine addition on workability of concrete was evaluated from slump cone test IS 1199-1959 [24]. According to the suggested range of workability of concrete in IS 456-



Figure 5. Test setup for concrete stress strain relationship under uniaxial compression loading

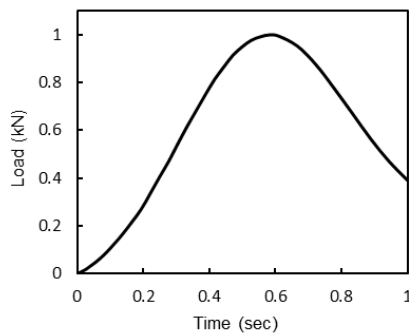


Figure 6. Normalized load vs time curve

2000 [15], a higher degree of workability was obtained for all seven mixes. The measured slump values are shown in Table 3. From the test results it was observed that, higher degree of workability to CM can be attributed to replacing 20% of cement with fly ash. The spherical shape of the fly ash particles lubricated the mix to achieve a high degree of workability with a negligible segregation [25]. Compared to CM at predetermined superplasticizer, water/binder ratio, and aggregate content, the percentage of alccofine adopted to replace the cement highly influenced the workability of concrete. Alccofine based mixes slump values linearly increased as its replacement percentage increased from 4 to 12%. This can be attributed to the enhanced plasticity of fresh concrete caused by increase in the specific surface area of total binder portion. Compared to cement, and fly ash particles, alccofine particles are highly fine with glassy surface characteristics. This is improved the specific surface area of the binder portion as replacement levels increased. Due to this, addition of alccofine enhanced the plasticity of fresh concrete and allowed the movement of constituent materials in the mix smoothly. All alccofine based mixes exhibited higher slump values without segregation and bleeding. With an increase in the percentage of alccofine, cohesiveness of mixes increased and setting time of mixes decreased. This was because of the availability of additional lime in overall binder mass.

### 3. 2. Mechanical Results

#### 3. 2. 1. Compressive Strength

The influence of alccofine on the compressive strength of concrete is shown in Table 3. From the test results it was observed that compared to the CM, alccofine based mixes achieved higher compressive strengths at 7, 28 and 56 days. The percentage increase in compressive strength of alccofine based mixes compared to CM is presented in Table 4. It was found that alccofine was advantageous up to a replacement level of 10% and thereafter, a fall in strength was noticed. However, it was found that the compressive strength of the specimens at 12 and 14% replacement levels were higher than CM. Until 10% of the replacement levels, the increase in strength was regular and then, as the replacement percentage increased, a reduction in strength was observed. The reason for increase in compressive strength can be attributed to the formation of additional network of C-S-H gel in the system, due to further hydration of cement together with pozzolanic actions of both fly ash and alccofine. Because of ultrafine particles and unique chemistry involved, the incorporation of alccofine resulted in the formation of dense matrix structure of the concrete. As alccofine is comprised with nearly 30% of lime, its replacement in place of cement has improved the formation of aluminates and silicates of calcium, to develop the portlandite during the hydration process to react with silica and provide an additional hydrated CSH gel network, which results in high strength to concrete at both early and later ages [11]. The reason for the reduction of compressive strength with the incorporation of alccofine in case of 12 and 14% replacement may be due to the unsoundness of the binder caused by the increase of free lime (CaO), magnesia (MgO) and alumina (Al<sub>2</sub>O<sub>3</sub>) which on hydration resulted in excessive expansion and formation of micro cracks thereby weakening the matrix of the specimens. This may result in an increase in the fragility of the specimens and show lower resistance to the compression load, thereby consequently decrease in strength was noticed.

TABLE 3. Compressive strength, Flexural strength and Split tensile strength test results (N/mm<sup>2</sup>)

Mix designation	Slump(mm)	Compressive strength			Flexural Strength			Split Tensile Strength		
		7days	28days	56days	7days	28days	56days	7days	28days	56days
M-C	120	56.23	68.33	71.77	4.76	5.27	5.68	4.45	5.01	5.16
M-AF4	131	58.93	69.47	72.83	5.12	5.61	5.83	4.69	5.18	5.36
M-AF6	140	61.57	74.13	76.90	5.28	5.70	6.01	4.97	5.31	5.65
M-AF8	148	63.53	76.20	78.37	5.50	5.85	6.12	5.12	5.47	5.98
M-AF10	159	65.27	80.33	82.97	5.70	6.22	6.33	5.23	5.81	6.12
M-AF12	168	62.57	77.35	78.77	5.58	6.02	6.15	4.93	5.49	5.76
M-AF14	163	61.37	72.27	75.13	5.02	5.65	5.85	4.61	5.13	5.32

**TABLE 4.** Increase in percentage of strength of alccofine based mixes compared to CM

Mix designation	Compressive strength (%)			Flexural Strength (%)			Split Tensile Strength (%)		
	7days	28days	56days	7days	28days	56days	7days	28days	56days
M-C	-	-	-	-	-	-	-	-	-
M-AF4	4.8	1.7	1.5	7.5	6.5	2.5	5.3	3.5	3.9
M-AF6	9.5	8.5	7.2	10.8	8.3	5.7	11.5	6.1	9.6
M-AF8	13.0	11.5	9.2	15.5	11.1	7.7	14.9	9.3	15.8
M-AF10	16.1	17.6	15.6	19.7	18.0	11.3	17.5	16.1	18.7
M-AF12	11.3	13.2	9.8	17.3	14.3	8.2	10.7	9.7	11.7
M-AF14	9.1	5.8	4.7	5.4	7.3	2.9	3.5	2.5	3.0

### 3. 2. 2. Flexural Strength

The influence of alccofine on the flexural strength of concrete is summarized in Table 3. It was observed from the results of the test that the flexural strength of concrete specimens follows a similar tendency to compressive strength. An incremental trend was observed up to 10% of cement replacement with alccofine at all ages. The percentage increase in flexural strength of alccofine based mixes compared to CM is presented in Table 4. The maximum flexural strength was exhibited by M-AF10 containing 10% alccofine compared to the CM and other alccofine based mixes irrespective of curing ages. Similar to compressive strength, in replacements beyond 10%, replacement the fall in flexural strength was observed in case of 12 and 14% replacements. However, in the present investigation, the obtained results evidently show that an increase in flexural strength values for alccofine based mixes were higher compared to CM. This is due to an improved performance of the binder material in terms of ability in binding the aggregates to strengthen the interfacial transition zone (ITZ) between aggregates and binder paste. The pozzolanic reaction of fly ash and alccofine resulted in strengthening the bond between aggregates and paste. The reduction in flexural strength is observed in cases of 12 and 14% replacements. The failure of flexural samples was accompanied by the opening of a single crack in the loading span along the depth of the specimen. Initially crack began in the interface region due to tensile strain produced by the compressive load and then micro crack extended into the concrete matrix. Under the flexural loading, the cracks are initiated in the interfacial zone at low stress and extended into the concrete matrix at higher stress and lead to the failure of the specimen at ultimate load. The failure specimens are shown in Figure 7(a).

### 3. 2. 3. Split Tensile Strength

The influence of alccofine on split tensile strength of concrete is presented in Table 3. The split tensile strength of the CM and alccofine based mixes showed a similar behavior like that of the compressive and flexural strengths. Among all 7 mixes, the highest split tensile strength was exhibited by

M-AF10 with 10% alccofine. The percentage increase in splitting tensile strength of alccofine based mixes compared to CM is presented in Table 4. It can be concluded from the test results that, all the alccofine based mixes showed greater split tensile strengths compared to the CM. But after 10% replacement, the increase in percentage of strength has reduced for mixes with 12 and 14% replacements. The failure pattern of the tested cylindrical specimens was shown in Figure 7(b). Under the splitting tensile strength test, the concrete specimens before attaining ultimate load, the internally developed microcracks proceeded outward from the maximum tension region of the cylinder towards the cylindrical surface with this clear vertical crack was appeared on the surface of cylindrical along the direction of loading. Initially these vertical cracks were appeared at top phase of the cylinder with further increase of load these vertical cracks travelled to bottom phase along the direction of the loading and led to failure of the specimen into two halves at ultimate load.

### 3. 2. 4. Relationship between Compressive Strength and Indirect Tensile Strength of Alccofine Based HSC

The compressive strength of concrete can be used to evaluate other engineering properties such as flexural strength and split tensile strength with the help of several proposed empirical relationships between the compressive strength and indirect tensile strength according to the code of practice and other earlier researchers [26-33]. The empirical relationships given in ACI 318-14 [34], IS 456-2000 [15] and earlier researcher's proposed relations presented in



**Figure 7.** Failure samples after testing (a) flexural strength (b) split tensile strength

Table 5 are used to predict flexural and split tensile strengths that are depicted in Figures 8 and 9, together with the proposed equation experimental values.

To assess the deviation between experimental flexural and split tensile strength and values computed using the proposed relation, IS 456-2000, ACI-318-14, and other empirical relations proposed by several researchers, an Integral Absolute Error (IAE) was performed and presented in Table 5, which can be expressed as follows:

$$IAE = \frac{\Sigma(A-B)}{\Sigma A} \times 100\% \tag{1}$$

where, A is actual value of split tensile strength / flexural strength; B is predicted values of split tensile strength / flexural strength.

From IAE it is clear that the proposed empirical relation showed lower error for both flexural and split tensile strengths than that of ACI-318, IS 456 and other empirical relations. In case of flexural strength, the assessed IAE by IS code [15] was close to IAE of the proposed relation. Ramadoss Perumal [31] proposed relation exhibited highest error compare to the proposed and other relationships. In case of split tensile strength the assessed IAE by Bhanja and Sengupta [29] and Rashid [28] relations were close to IAE of the proposed equation of present study. Oluokun [27] relation exhibited highest error compared to the proposed relation of the present study and other relations. From this it can be assured that the proposed relationship fits well with the experimental values that of the ACI and IS code and other researchers proposed equations. This indicates the highest precision in the predicted relationships.

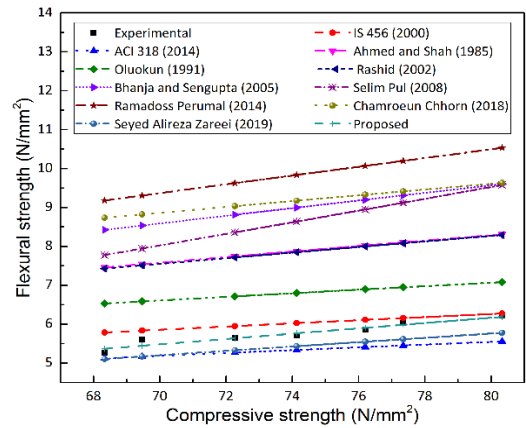


Figure 8. Relationship between flexural strength and compressive strength

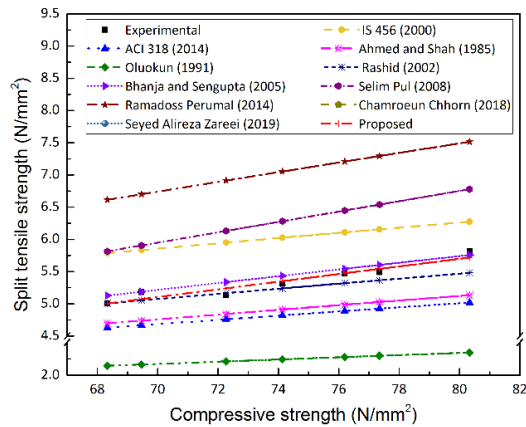


Figure 9. Relationship between split tensile strength and compressive strength

TABLE 5. The empirical relations between flexural strength and compressive strength, split tensile strength and compressive strength and corresponding IAE

Code of practice /researcher	Empirical relation		Integral Absolute Error (IAE) (%)	
	Flexural Strength	Split Tensile Strength	Flexural Strength	Split Tensile Strength
Proposed	$f_{fs} = 0.136f_{ck}^{0.87}$	$f_{sts} = 0.157f_{ck}^{0.82}$	3.29	3.32
ACI-318-14 (2014) [34]	$f_{fs} = 0.62(f'_c)^{0.5}$ for $f'_c < 83MPa$	$f_{sts} = 0.56(f'_c)^{0.5}$ for $f'_c < 83MPa$	8.33	10.86
IS-456-2000 [15]	$f_{fs} = 0.7f_{ck}^{0.5}$	$f_{sts} = 0.7f_{ck}^{0.5}$	3.69	11.42
Ahmed and Shah (1985) [26]	$f_{fs} = 0.44(f'_c)^{0.67}$ for $f'_c < 84MPa$	$f_{sts} = 0.46(f'_c)^{0.55}$ for $f'_c < 84MPa$	34.19	9.41
Oluokun et al. (1991) [27]	$f_{fs} = 0.79(f'_c)^{0.5}$	$f_{sts} = 0.21(f'_c)^{0.55}$	16.80	58.64
Rashid et al. (2002) [28]	$f_{fs} = 0.42(f'_c)^{0.68}$ for $5 < f'_c < 120MPa$	$f_{sp} = 0.47(f'_c)^{0.56}$ for $5 < f'_c < 120MPa$	33.67	3.91
Bhanja and Sengupta (2005) [29]	$f_{fs} = 0.275(f'_c)^{0.81}$	$f_{sp} = 0.248(f'_c)^{0.717}$	52.30	3.45
Selim Pul (2008) [30]	$f_{ft} = 0.034f_c^{1.286}$	$f_{sp} = 0.106f_c^{0.948}$	43.36	13.80
Ramadoss Perumal (2014) [31]	$f_{fs} = 0.252(f'_c)^{0.851}$	$f_{sts} = 0.235(f'_c)^{0.79}$	66.20	28.66
Chamroen Chhorn (2018) [32]	$f_{ft} = 0.678f_{ck}^{0.605}$	$f_{sp} = 0.47f_c^{0.511}$	56.76	21.60
Seyed Alireza Zareei (2019) [33]	$f_{ft} = 0.0558f_{ck} + 1.2966$	$f_{sp} = 0.0539f_{ck} + 0.1531$	7.70	24.86

Where  $f'_c$  is the Cylindrical compressive strength,  $f_{ck}$  is the Cube compressive strength

**3. 3. Water Absorption and Porosity** The water absorption and porosity results are presented in Figure 10. The water absorption and porosity for the CM is found to be 2.95 and 4.95%. In the case of mixes containing alccofine, water absorption and porosity gradually decreased at an average rate of 35.42 and 31.11% with respect to replacement levels from 4 to 10%. Thereafter, for replacement levels of 12 and 14%, water absorption and porosity increased compared to the 10% replacement level. An increase in the percentage of water absorption and porosity for the replacement of 12% compared to the replacement of 10% was around 1.7 and 24.65%. In the case of 14%, it was approximately 43.38% for water absorption and 43.23% for porosity. Compared with CM, all mixes containing alccofine showed lower water absorption and porosity. The reduction in water absorption and porosity up to 10% replacement can be attributed to higher consistency and density of the binder paste due to the inclusion of alccofine and higher bond strength between the binder and the aggregates, thereby plummeting the micro pore in the hardened concrete. The reason for the increase in water absorption and the porosity for replacements of 12 and 14% compared to the 10% replacement may be due to the presence of unreacted lime that might have developed the small micro cracks in the hardened concrete matrix.

**3. 4. Uniaxial Compressive Stress Strain Behavior** The average of three specimens data collected from the DAC system is used to plot the stress-strain curves for each mixture at 28-days strength and is shown in Figure 11. The load on specimen increased at a higher rate in the initial stages up to 75% of its ultimate load and up to ultimate load the rate of increase in load was slow. The test on specimen continued until load dropped by 60-65% of the ultimate load. During the test it was observed that the vertical cracks distributed around the specimens were

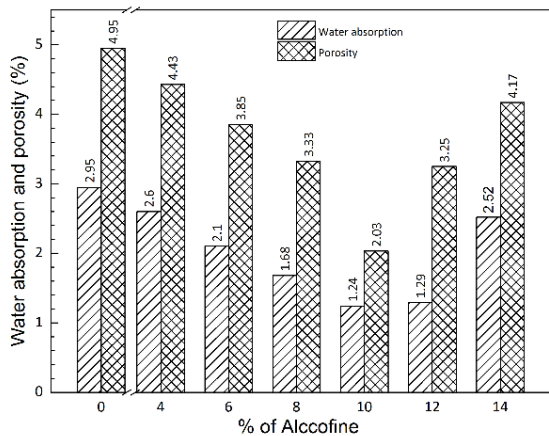


**Figure 10.** Influence of alccofine on water absorption and porosity of HSC

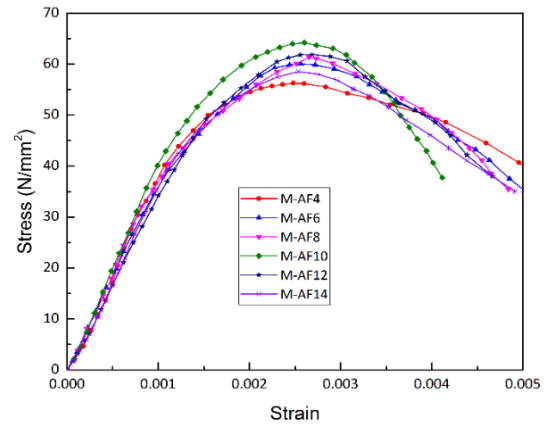


**Figure 11.** Influence of alccofine on stress strain behavior of HSC

noticed on the specimen with increase in the load. The cracks propagated from the bottom phase to the top phase of the specimen with further increase of load. The initial cracks on the specimens were appeared around 80-85% of the ultimate load. Crack propagation and crack width increased after ultimate load. The rate of decrease of load after the peak (in descending portion of stress-strain curve) was faster due to rapid crack growth. This led the failure of the specimen once it reached its maximum failure strain.

**3. 4. 1. Young's Modulus** Due to the enhancement in compressive strength of concrete by addition of alccofine, the change in Young's modulus of the mixes has been analyzed. The Young's modulus of HSC was determined using the ASTM C469 standards [22]. The empirical relation given in ACI 318 and IS 456 was used to assess the Young's modulus from experimental compressive strength and same is presented in Figure 12 in comparison with determined Young's modulus from stress-strain curves.

The calculated experimental Young's modulus values followed a similar tendency as compressive strength. Compared to CM, alccofine based mixes have higher Young's modulus except the mix with 12% replacement. The percentage increase in Young's modulus with respect to CM is 2.91, 3.23, 8.66, 11.09, and 0.45% for the replacements of 4, 6, 8, 10 and 14%, respectively. The Young's modulus values may increase due to the lower porosity of the interfacial transition zone and the presence of significant amount of unreacted fly ash particles which may act as fine aggregate [35]. The Young's modulus values predicted from ACI 318 and IS 456 are showed similar observation as those obtained from experimentation. The Young's modulus values predicted using ACI code relation was comparable with experimental values than IS code predicted values. IS code recommended equation predicted higher Young's modulus than experimental values.

**3. 4. 2. Energy Absorption Capacity (EAC)** From Figure 11, it can be observed that as alccofine replacement levels increased from 4 to 10%, the compressive strength and compressive strains increased compared to control mix. The larger linear portion of the stress strain curves were existed as the as alccofine replacement levels increased. This indicates an increase in brittleness of the concrete. In order to understand this, EAC of the all the mixes were analyzed. The calculated EAC in terms of  $\text{Joule/m}^3$  is presented in Figure 13. From the results obtained, it can be said that the EAC of alccofine-based mixes was decreased due to incorporation of alccofine. All the alccofine based mixes have lower EAC than control mix. This was attributed by an increase in compressive strength of the mixes due to incorporation of alccofine. from EAC results, it can be concluded that incorporation of alccofine led to an increase in brittle behavior of the concrete. The percentage of decrease in EAC with respect to the replacement of alccofine is approximately 1.608, 5.461, 7.716, 17.697, 11.351 and 10.283% for the replacements

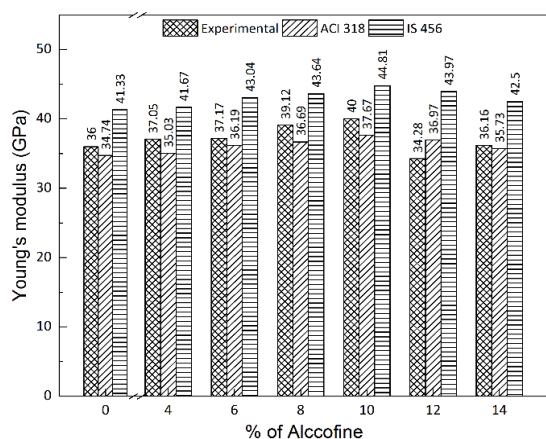


**Figure 12.** Influence of alccofine on Young's modulus of HSC

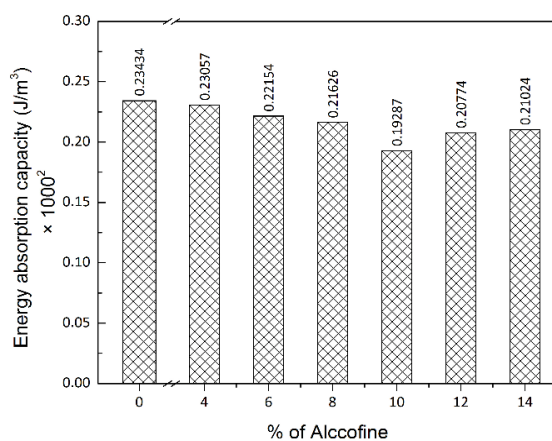


**Figure 13.** Influence of alccofine on Energy absorption capacity of HSC

of 4, 6, 8, 10, 12 and 14%, respectively. At a replacement level of 10%, the specimens showed lowest EAC than that of control mix and other alccofine based mixes. This was due to higher compressive strength and brittleness of the mix.

#### 4. CONCLUSIONS

In this paper, the feasibility of developing HSC using partial replacement of cement with alccofine with fly ash combination was investigated. The use of alccofine with combination of fly ash proves to be advantageous in development of HSC. Water content required to achieve desired workability can be reduced as alccofine incorporation increased workability of concrete at a predetermined superplasticizer content and water-binder ratio. Addition of alccofine decreased setting time of concrete compared to CM; this is advantageous in early removal of formwork in constructions. At cement replacement with 10% alccofine and 20% fly ash exhibited HSC with highest compressive, flexural and split tensile strengths at 7, 28, and 56-days compared to CM and other alccofine based mixes. The beneficial effect of alccofine began to weaken after 10% incorporation. Water absorption and porosity of HSC decreased with incorporation of alccofine compared CM. Mix with 10% alccofine exhibited highest Young's modulus. The predicted experimental Young's modulus from uniaxial stress-strain behavior of concrete was comparable with predicted Young's modulus from ACI code relation than from IS code relation. Based on experimental compressive strength results, empirical relations were proposed to predict the flexural and split tensile strengths. From the predicted IAE, the proposed empirical relation in this paper was found with lowest IAE (3.29 and 3.32% for flexural strength and split tensile strengths) than the ACI 318, IS 456 and other proposed relations of researchers.

#### 5. REFERENCES

1. Phul, A.A., Memon, M.J., Shah, S.N.R. and Sandhu, A.R., "Ggbs and fly ash effects on compressive strength by partial replacement of cement concrete", *Civil Engineering Journal*, Vol. 5, No. 4, (2019), 913-921.
2. Biswas, R. and Rai, B., "Efficiency concepts and models that evaluates the strength of concretes containing different supplementary cementitious materials", *Civil Engineering Journal*, Vol. 5, No. 1, (2019), 18-32.
3. Fallah, S. and Nematzadeh, M., "Mechanical properties and durability of high-strength concrete containing macro-polymeric and polypropylene fibers with nano-silica and silica fume", *Construction and Building Materials*, Vol. 132, (2017), 170-187.
4. Shannag, M., "High strength concrete containing natural pozzolan and silica fume", *Cement and Concrete Composites*, Vol. 22, No. 6, (2000), 399-406.

5. Çımar, M., Karpuzcu, M. and Çanakçı, H., "Effect of waste marble powder and fly ash on the rheological characteristics of cement based grout", *Civil Engineering Journal*, Vol. 5, No. 4, (2019), 777-788.
6. Gamil, Y., Bakar, I. and Ahmed, K., "Simulation and development of instrumental setup to be used for cement grouting of sand soil", *Emerging Science Journal*, Vol. 1, No. 1, (2017), 16-27.
7. Ekeleme, A.C. and Agunwamba, J.C., "Experimental determination of dispersion coefficient in soil", *Emerging Science Journal*, Vol. 2, No. 4, (2018), 213-218.
8. Sharma, D., Sharma, S. and Goyal, A., "Utilization of waste foundry slag and alccofine for developing high strength concrete", *International Journal of Electrochemical Science*, Vol. 11, No. 1, (2016), 3190-3205.
9. HS, M.A. and Kshirsagar, S., "Use of alccofine 1203 in concrete roads", *International Journal of Applied Engineering Research*, Vol. 13, No. 7, (2018), 299-301.
10. Singhal, D., Junaid, M.T., Jindal, B.B. and Mehta, A., "Mechanical and microstructural properties of fly ash based geopolymer concrete incorporating alccofine at ambient curing", *Construction and Building Materials*, Vol. 180, (2018), 298-307.
11. Gupta, A.K., "Experimental study of strength relationship of concrete cube and concrete cylinder using ultrafine slag alccofine", *International Journal of Scientific & Engineering Research*, vol. 5, (2014), 102-107.
12. Narender Reddy, A. and Meena, T., "An experimental investigation on mechanical behaviour of eco-friendly concrete", in *Materials Science and Engineering Conference Series*. Vol. 263, (2017), 032010.
13. IS, Indian standard ordinary portland cement, 43 grade-specification, Bureau of Indian Standards, New Delhi, (2003).
14. IS, Indian standard pulverized fuel ash-specification, Bureau of Indian Standards, New Delhi, (2003).
15. BIS, I., 456 plain and reinforced concrete-code of practice", Bureau of Indian Standards, New Delhi, (2000).
16. Is:12089-1987, specification for granulated slag for the manufacture of portland slag cement, Bureau of Indian Standards, New Delhi, (1987).
17. BIS, Is 383-1970: Specification for coarse and fine aggregate from natural sources for concrete (second rev.), Bureau of Indian Standards, New Delhi, (1970).
18. Is:9103-1999, concrete admixture-specifications, Bureau of Indian Standards, New Delhi, (1999).
19. Is 10262: 2009, concrete mix proportioning guidelines, Bureau of Indian Standards, New Delhi, (2009).
20. Is:516-2004, "methods of test for strength of concrete, Bureau of Indian Standards, New Delhi, (2004).
21. -IS, Splitting tensile strength of concrete-method of test. Bureau of Indian Standards, New Delhi, (1999).
22. Standard, A., C469, 2010, "standard test method for static modulus of elasticity and poisson's ratio of concrete in compression." astm international, west conshohocken, pa, (2010), doi: 10.1520/c0469\_c0469m-10.
23. ASTM, C., "Standard test method for density, absorption, and voids in hardened concrete", C642-13, (2013).
24. Is, Methods of sampling and analysis of concrete, Bureau of Indian Standards, New Delhi, (2004).
25. Mehta, P.K. and Monteiro, P.J., *Concrete microstructure, properties and materials*, (2017).
26. Ahmad, S.H. and Shah, S.P., "Structural properties of high strength concrete and its implications for precast prestressed concrete", *PCI Journal*, Vol. 30, No. 6, (1985), 92-119.
27. Oluokun, F., "Prediction of concrete tensile strength from its compressive strength: An evaluation of existing relations for normal weight concrete", *Materials Journal*, Vol. 88, No. 3, (1991), 302-309.
28. Rashid, M., Mansur, M. and Paramasivam, P., "Correlations between mechanical properties of high-strength concrete", *Journal of Materials in Civil Engineering*, Vol. 14, No. 3, (2002), 230-238.
29. Bhanja, S. and Sengupta, B., "Influence of silica fume on the tensile strength of concrete", *Cement and concrete research*, Vol. 35, No. 4, (2005), 743-747.
30. Pul, S., "Experimental investigation of tensile behaviour of high strength concrete", *Indian Journal of Engineering and Materials Sciences*, Vol. 15, (2008), 467-472.
31. Perumal, R., "Correlation of compressive strength and other engineering properties of high-performance steel fiber-reinforced concrete", *Journal of Materials in Civil Engineering*, Vol. 27, No. 1, (2015), 04014114.
32. Chhorn, C., Hong, S.J. and Lee, S.W., "Relationship between compressive and tensile strengths of roller-compacted concrete", *Journal of Traffic and Transportation Engineering (English Edition)*, Vol. 5, No. 3, (2018), 215-223.
33. Zareei, S.A., Ameri, F., Bahrami, N., Shoaee, P., Moosaei, H.R. and Salemi, N., "Performance of sustainable high strength concrete with basic oxygen steel-making (BOS) slag and nano-silica", *Journal of Building Engineering*, Vol. 25, (2019), 100791.
34. 318, A.C., "Building code requirements for structural concrete (aci 318-14)[and] commentary on building code requirements for structural concrete (aci 318-14), (2014).

### Persian Abstract

#### چکیده

استفاده از مواد افزودنی نکمیلی سیمان (SCM) در ساخت بتن به عنوان یک مزیت مالی، فنی و زیست‌محیطی در نظر گرفته شده است. در همین راستا، این مقاله به بررسی تجربی و تحلیلی بتن با استحکام بالا (HSC) با آلکوفین-۱۲۰۳ (آلکوفین) و خاکستر به عنوان جایگزین بخشی از سیمان می‌پردازد. در مجموع هفت مخلوط با درصد‌های مختلف آلکوکسین (۱۴-٪/۴) تهیه شد. مخلوط بتن آماده شده به طور تجربی برای استحکام کششی لاغری، فشاری، خمشی و تقسیم‌شده در سنین ۷، ۲۸ و ۵۶ روزه مورد آزمایش قرار گرفت. رفتار استرس محور یک محوره، و جذب آب و تخلخل در سن پخت ۲۸ روزه بررسی شد. مدول یونگ، ظرفیت جذب انرژی (EAC) و خطای مطلق انتگرال (IAE) به روش تحلیلی مورد بررسی قرار گرفت. از نتایج آزمون، مشاهده شد که جایگزینی سیمان با آلکسوفین به طور قابل توجهی کارایی بتن را بهبود می‌بخشد. در بین تمام مخلوط‌ها، مخلوط با ۱۰٪ محتوای آلکوفین رفتار بهتری در تمام پارامترهای مورد بررسی نشان داد. اختلاط آلکوفین تأثیر منفی بر رفتار HSC فراتر از ۱۰٪ جایگزینی در کلیه پارامترهای مورد بررسی نشان داد. بر اساس نتایج مقاومت فشاری تجربی، روابط تجربی برای پیش‌بینی مقاومت کششی خمشی و شکافته پیشنهاد شده است. روابط تجربی ارائه شده دارای کمترین IAE (۲۹/۳ و ۳۲/۳) برای مقاومت کششی خمشی و تقسیم‌شده در مقایسه با IS 456، ACI-318 و روابط تجربی است که توسط محققان قبلی ارائه شده است.